

8. N. N. Mirol'yubov, M. V. Kostenko, M. L. Levinshtein, and N. I. Tikodeev, Methods of Electrostatic Field Calculation [in Russian], Vysshaya Shkola, Moscow (1963).
9. K. E. Leonhard and E. H. Hyde, Cryo. Tech., 7, No. 1 (1971).

## A RHEOLOGICAL MODEL OF A THIXOTROPIC VISCOELASTOPLASTIC MEDIUM

G. Ya. Kunnos, V. M. Vasilevskii,  
and V. É. Mironov

UDC 532.135:536.242

A model is proposed which allows for the difference between instantaneous and slow deformations during loading and unloading (of a mixture based on mineral binding substances). At different constant deformation rates the model reflects the dependence of the relaxation phenomena on the velocity and describes the thixotropy loop.

In our investigations of the rheological properties of foam - concrete mixtures by the creep method under simple shear [1] and in the same medium (adobe) at a more mature age under axial compression and tension [2], as well as under simple shear in the presence or absence of normal stress [3-5], the difference between the instantaneous and slow deformations during loading and unloading was clearly and reliably traced. Therefore, we proposed a new rheological element, a ratchet with an imperfection, which can be called a generalized St. Venant element [1-5]. For the rheological description of media possessing fluidity this element is connected to the Schofield - Scott-Blair model as shown in Fig. 1; the series connection of the second Newton - St. Venant element to the indicated model provides the function  $\dot{\gamma} = f(\tau)$  with a piecewise-linear character [1] by which we approximate the nonlinear fluidity curve.

When  $\tau_c < \tau < \tau_d$  the equation of state of the model during loading, i.e., when the generalized St. Venant elements do not come into play, has the form

$$\tau - \tau_0 + \frac{\eta_1}{\eta_3} (\tau - \tau_c) + \left[ n_1 + n_2 \left( 1 + \frac{\eta_1}{\eta_2} + \frac{\eta_1}{\eta_3} \right) \right] \dot{\tau} + n_1 n_2 \ddot{\tau} = \eta_1 \dot{\gamma} + \eta_1 n_2 \ddot{\gamma}. \quad (1)$$

When  $\tau_0 < \tau < \tau_c$  the second term and  $n_2 \eta_1 / \eta_3$  drops out of the left-hand side of Eq. (1).

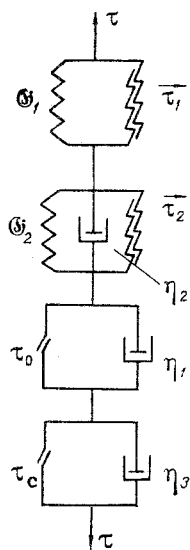


Fig. 1. Rheological model of a thixotropic medium with a nonlinear fluidity characteristic.

## Constant Stress and Unloading

Solving Eq. (1) with  $\tau = \text{const}$  ( $\tau_c < \tau < \tau_d$ ) and the initial conditions

$$t = 0, \quad \gamma(0) = \frac{\tau}{\mathfrak{G}_1}, \quad (2)$$

$$t = 0, \quad \dot{\gamma}(0) = \frac{\tau}{\eta_2} + \frac{\tau - \tau_0}{\eta_1} + \frac{\tau - \tau_c}{\eta_3},$$

we obtain

$$\gamma = \frac{\tau}{\mathfrak{G}_1} + \frac{\tau}{\mathfrak{G}_2} \left[ 1 - \exp\left(-\frac{t}{n_2}\right) \right] + \frac{\tau - \tau_0}{\eta_1} t + \frac{\tau - \tau_c}{\eta_3} t. \quad (3)$$

When  $\tau_0 < \tau < \tau_c$  the last term falls out of Eq. (3) (the solution of the equation of the Schofield-Scott-Blair model).

Solving the equation  $\dot{\gamma} + n_2 \ddot{\gamma} = 0$  to establish the law of reverse fluidity after unloading with  $\tau = \tau_1$ , and using the initial conditions

$$t = t_1, \quad \gamma(t_1) = \frac{\tau_1}{\mathfrak{G}_1} + \frac{\tau_2}{\mathfrak{G}_2} \frac{\tau - \tau_1}{\mathfrak{G}_1} + \frac{\tau - \tau_0}{\eta_1} t_1 + \frac{\tau - \tau_c}{\eta_3} t_1, \quad (4)$$

$$t = t_1, \quad \dot{\gamma}(t_1) = -\frac{\tau - \tau_2}{\eta_2},$$

we obtain

$$\gamma(t - t_1) = \frac{\tau - \tau_2}{\mathfrak{G}_2} \exp\left(-\frac{t - t_1}{n_2}\right) + \frac{\tau_1}{\mathfrak{G}_1} + \frac{\tau_2}{\mathfrak{G}_2} + \frac{\tau - \tau_0}{\eta_1} t_1 + \frac{\tau - \tau_c}{\eta_3} t_1, \quad (5)$$

where the first term denotes the inverse fluidity while the others denote the residual deformation. As follows from (5), the residual deformation of the medium is caused by two deformation mechanisms, viscoplastic deformation and the plastic deformation proper, inherent to a solid body and described using the generalized St. Venant element.

To determine the 13 rheological characteristics of the model shown in Fig. 1 (its nine parameters and the characteristics  $\mathfrak{G}_\infty$ ,  $n_1$ ,  $n_2$ , and  $\eta^*$  which depend on them) one must use the dependences  $\gamma(t) = f(\tau)$  ( $\tau = \text{const}$ ) and  $\dot{\gamma} = \varphi(\tau)$  ( $\dot{\gamma} = \text{const}$ ).

The values of  $\mathfrak{G}_1$ ,  $\mathfrak{G}_2$ ,  $\mathfrak{G}_\infty$ ,  $\eta_1$ ,  $\eta_2$ ,  $n_1$ ,  $n_2$ ,  $\tau_0$ , and  $\tau_c$  are determined by the generally known methods. The four remaining characteristics can be calculated from the dependences

TABLE 1. Numerical Values of Rheological Characteristics of a Gas-Concrete Mixture at the Moment of Maximum Swelling Rate at Different Temperatures

Plasticity characteristics						
swelling temp., °C	time after pouring, min	$\tau_0$	$\tau_c$	$\tau_1$	$\tau_2$	
		Pa				
40	16	570	1350	1100	716	
50	8	670	1050	388	293	
60	3	120	760	—	—	
Viscosity characteristics						
swelling temp., °C	time after, pouring, min	$\eta_1$	$\eta_2$	$\eta^*$	$\eta_3$	
		Pa·sec				
40	16	$4,20 \cdot 10^5$	$10 \cdot 10^4$	$3,85 \cdot 10^4$	$4,26 \cdot 10^4$	
50	8	$0,96 \cdot 10^5$	$8,39 \cdot 10^4$	$1,52 \cdot 10^4$	$1,82 \cdot 10^4$	
60	3	$0,60 \cdot 10^5$	—	$0,26 \cdot 10^4$	$0,27 \cdot 10^4$	
Elasticity, relaxation, and retardation characteristics						
swelling temp., °C	time after pouring, min	$\mathfrak{G}_1$	$\mathfrak{G}_2$	$\mathfrak{G}_\infty$	$n_1$	$n_2$
		Pa			sec	
40	16	$3,56 \cdot 10^4$	$3,40 \cdot 10^4$	$1,74 \cdot 10^4$	11,8	2,95
50	8	$2,46 \cdot 10^4$	$1,84 \cdot 10^4$	$1,05 \cdot 10^4$	3,9	4,56

$$\eta^* = \frac{\tau - \tau_c}{\dot{\gamma}_{est II}}; \quad \frac{1}{\eta^*} = \frac{1}{\eta_1} + \frac{1}{\eta_2}; \quad \dot{\tau}_1 = \tau - \mathfrak{G}_1 \dot{\gamma}_3; \quad \dot{\tau}_2 = \tau - \mathfrak{G}_2 \dot{\gamma}_4. \quad (6)$$

An example of the rheological characteristics which we investigated is given in Table 1.

From an analysis of Table 1 it is seen, first, that a gas-concrete mixture, in varying  $\dot{\gamma}$  by about an order of magnitude, possesses a relatively low consistency, characterized by the "degree of structure destruction," i.e., by the ratio  $\eta_1/\eta_3$ , which lies in the range of 10-15. Second, it is established that in the range of temperature variation the values of the rheological characteristics decrease markedly with a decrease in temperature, which agrees with the concepts of the molecular-kinetic theory in application to its use in deformation processes.

A Constant Deformation Rate ( $\dot{\gamma} = \text{const} = v$ ) upon a  
(Stepwise) Increase in Velocity

a) For  $\tau_0 < \tau < \tau_c$  we have the equation

$$\tau - \tau_0 + \left[ n_1 + n_2 \left( 1 + \frac{\eta_1}{\eta_2} \right) \right] \dot{\tau} + n_1 n_2 \ddot{\tau} = \eta_1 v. \quad (7)$$

Taking  $\tau - \tau_0 = \exp(\alpha t)$ , we obtain the characteristic equation of the homogeneous differential equation and the values of its roots:

$$1 + \left[ n_1 + n_2 \left( 1 + \frac{\eta_1}{\eta_2} \right) \right] \alpha + n_1 n_2 \alpha^2 = 0, \quad (8)$$

$$\alpha_{1,2} = \frac{- \left[ n_1 + n_2 \left( 1 + \frac{\eta_1}{\eta_2} \right) \right] \pm \sqrt{\left[ n_1 + n_2 \left( 1 + \frac{\eta_1}{\eta_2} \right) \right]^2 - 4 n_1 n_2}}{2 n_1 n_2}. \quad (9)$$

We introduce the designations

$$\alpha_1 = -\frac{1}{n_1^*}; \quad \alpha_2 = -\frac{1}{n_2^*}. \quad (10)$$

Using the solution of (7)

$$\tau = \tau_0 + C_1 \exp\left(-\frac{t}{n_1^*}\right) + C_2 \exp\left(-\frac{t}{n_2^*}\right) + \eta v \quad (11)$$

and the initial conditions

$$t = 0, \quad \tau(0) = 0, \quad \dot{\tau}(0) = \mathfrak{G}_\infty v, \quad (12)$$

we arrive at the expression

$$\begin{aligned} \tau = \tau_0 - \left[ \frac{n_1^* n_2^*}{n_2^* - n_1^*} \left( \mathfrak{G}_\infty v - \frac{1}{n_1^*} \tau_0 - \frac{1}{n_1^*} \eta_1 v \right) + \tau_0 + \eta_1 v \right] \exp\left(-\frac{t}{n_1^*}\right) \\ + \frac{n_1^* n_2^*}{n_2^* - n_1^*} \left( \mathfrak{G}_\infty v - \frac{1}{n_1^*} \tau_0 - \frac{1}{n_1^*} \eta_1 v \right) \exp\left(-\frac{t}{n_2^*}\right) + \eta_1 v. \end{aligned} \quad (13)$$

b) For  $\tau_c < \tau < \tau_d$  we have an equation obtained after obvious transformations of (1):

$$\tau - \tau_c + \left( \frac{\eta_3}{\mathfrak{G}_1} + \frac{\eta_2 \eta_3}{\mathfrak{G}_2 \eta_1} + \frac{\eta_3}{\mathfrak{G}_2} + \frac{\eta_2}{\mathfrak{G}_2} \right) \dot{\tau} + \frac{\eta_3 \eta_2}{\mathfrak{G}_1 \mathfrak{G}_2} \ddot{\tau} = \eta_3 \dot{\gamma} + \eta_3 n_2 \ddot{\gamma}. \quad (14)$$

Taking  $\tau - \tau_c = \exp(\alpha t)$ , we represent the characteristic equation and its roots in the form

$$1 + \left( \frac{\eta_3}{\mathfrak{G}_1} + \frac{\eta_2 \eta_3}{\mathfrak{G}_2 \eta_1} + \frac{\eta_3}{\mathfrak{G}_2} + n_2 \right) \alpha + \frac{\eta_3 n_2}{\mathfrak{G}_1} \alpha^2 = 0, \quad (15)$$

$$\alpha_{3,4} = \left\{ - \left( \frac{\eta_3}{\mathfrak{G}_1} + \frac{n_2 \eta_3}{\eta_1} + \frac{\eta_3}{\mathfrak{G}_2} + n_2 \right) \pm \sqrt{\left( \frac{\eta_3}{\mathfrak{G}_1} + \frac{n_2 \eta_3}{\eta_1} + \frac{\eta_3}{\mathfrak{G}_2} + n_2 \right)^2 - 4 \frac{n_2 \eta_3}{\mathfrak{G}_1}} \right\} \left( 2 \frac{\eta_3 n_2}{\mathfrak{G}_1} \right)^{-1}. \quad (16)$$

We introduce the designations

$$\alpha_3 = -\frac{1}{n_3^*}; \quad \alpha_4 = -\frac{1}{n_4^*}. \quad (17)$$

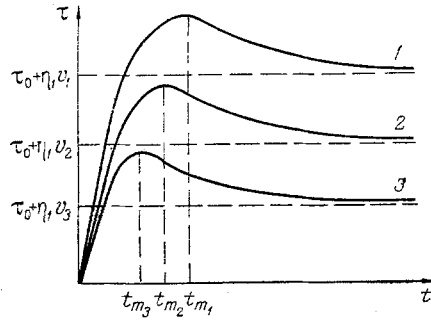


Fig. 2. Dependence of shear stress on deformation time (deformation) for a viscoelastoplastic medium described by the model of Fig. 1,  $v_1 > v_2 > v_3$ .

Proceeding as in case a), i.e., using the solution of Eq. (14) in the form  $\tau = \tau_c + C_3 \exp\left(-\frac{t}{n_3^*}\right) + C_4 \exp\left(-\frac{t}{n_4^*}\right) + \eta_3 v$  and the initial conditions

$$t = 0, \quad \tau(0) = \tau_c, \quad \dot{\tau}(0) = \mathfrak{G}_\infty v, \quad (18)$$

we obtain the expression

$$\tau = \tau_c - \left[ \frac{n_3^* n_4^*}{n_4^* - n_3^*} \left( \mathfrak{G}_\infty v + \frac{\eta_3}{n_3^*} v \right) + \eta_3 v \right] \exp\left(-\frac{t}{n_3^*}\right) + \frac{n_3^* n_4^*}{n_4^* - n_3^*} \left( \mathfrak{G}_\infty v + \frac{\eta_3}{n_3^*} v \right) \exp\left(-\frac{t}{n_4^*}\right) + \eta_3 v. \quad (19)$$

Let us analyze the character of the dependence  $\tau(t) = f(v)$  on the example of (13) by investigating (11) at the maximum. Equating the derivative of (11) to zero, we obtain

$$\exp\left(\frac{n_2^* - n_1^*}{n_1^* n_2^*} t_m\right) = -\frac{C_1 n_2^*}{C_2 n_1^*},$$

from which

$$t_m = \frac{n_1^* n_2^* \ln\left(-\frac{C_1 n_2^*}{C_2 n_1^*}\right)}{n_2^* - n_1^*}. \quad (20)$$

Substituting  $C_1$  and  $C_2$  from (11), by using (12) we can ascertain that

$$t_m = n_1^* n_2^* (n_2^* - n_1^*)^{-1} \left\{ \ln \left[ \frac{n_1^* n_2^*}{n_2^* - n_1^*} \left( \mathfrak{G}_\infty v - \frac{\tau_0}{n_1^*} - \frac{\eta_1 v}{n_1^*} + \tau_0 + \eta_1 v \right) \right] - \ln \left[ \frac{n_1^* n_2^*}{n_2^* - n_1^*} \left( \mathfrak{G}_\infty v - \frac{\tau_0}{n_1^*} - \frac{\eta_1 v}{n_1^*} \right) \right] \right\}. \quad (21)$$

We find the value of the maximum stress  $\tau_{\max}$  at  $t = t_m$  by replacing  $t$  by  $t_m$  in (13).

The character of the dependence  $\tau = \tau(t)$  is presented in Fig. 2, from which it is seen that  $t_{m_1}(v_1) > t_{m_2}(v_2) > t_{m_3}(v_3)$  and  $\tau_{\max}(v_1) > \tau_{\max}(v_2) > \tau_{\max}(v_3)$  when  $v_1 > v_2 > v_3$ . Such a picture fully corresponds to propositions known from fundamental work on rotary viscosimetry, such as [6], for liquidlike systems and elastic liquids, and for viscoelastoplastic media in a certain range of values of  $\dot{\gamma} = \text{const} = v$ , not too low and not too high. As seen from Fig. 2, one does not observe a monotonic rise of the function  $\tau(t)$  without extrema for  $\dot{\gamma} = \text{const}$ , characteristic for relaxation phenomena in a medium described by the Shvedov - Bingham model. It is seen from Eq. (13) that a monotonic character (without a maximum) for the function  $\tau(t)$ , or, which is the same thing,  $\tau(\dot{\gamma})$ , is theoretically possible only for vanishingly low values of  $v$ . Moreover, it follows from (13) and (19) that both relaxation and retardation mechanisms, inherent to the model proposed by us [1], take part in the extremal dependence  $\tau(t)$ , which follows from the presence of the terms  $n_1$  and  $n_2$  in these expressions.

The procedure for determining the five independent rheological characteristics of Eq. (13) and the six characteristics of Eq. (19) consists in the five- and six-fold variation of  $\dot{\gamma} = \text{const} = v$  and the solution of the system of algebraic equations using computer technology.

#### A Constant Deformation Rate ( $\dot{\gamma} = \text{const} = v$ ) upon a (Stepwise) Decrease in Velocity

Upon a stepwise or smooth decrease in  $\dot{\gamma}$ , the elements  $\bar{\tau}_1$  and  $\bar{\tau}_2$  enter into the work. For the first unloading variant (Fig. 3a), allowing for the fact that  $AB = \tau_3 - \tau_c$ , after simple geometrical transformations we obtain

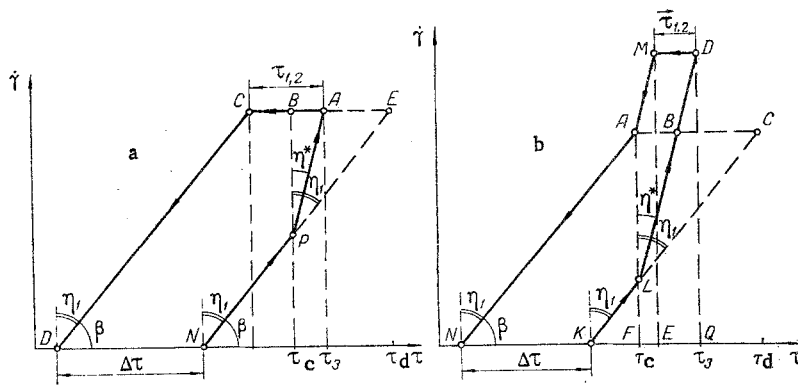


Fig. 3. Area of thixotropy loop: a) for  $|\vec{\tau}_{1,2}| > |\tau_3 - \tau_c|$ ; b) for  $|\vec{\tau}_{1,2}| < |\tau_3 - \tau_c|$ .

$$BP = \frac{AB}{\eta^*} = \frac{\tau_3 - \tau_c}{\eta^*};$$

$$BE = BP \eta_1 = \frac{\eta_1}{\eta^*} (\tau_3 - \tau_c);$$

$$AE = BE - AB = (\tau_3 - \tau_c) \left( \frac{\eta_1}{\eta^*} - 1 \right) = \frac{\eta_1}{\eta_3} (\tau_3 - \tau_c),$$

where  $\eta^*$  is determined from (6) and

$$\Delta\tau = CE = \vec{\tau}_1 + \frac{\eta_1}{\eta_3} (\tau_3 - \tau_c). \quad (22)$$

With allowance for (22), in accordance with Eq. (1) transformed for the section  $\tau_0 < \tau < \tau_c$  (see Fig. 3), the equation of the problem has the form

$$\tau - \tau_0 + \vec{\tau}_{1,2} + \frac{\eta_1}{\eta_3} (\tau_3 - \tau_c) + \left[ n_1 + n_2 \left( 1 + \frac{\eta_1}{\eta_2} \right) \right] \dot{\tau} + n_1 n_2 \ddot{\tau} = \eta_1 v. \quad (23)$$

Taking

$$\tau - \tau_0 + \vec{\tau}_{1,2} + \frac{\eta_1}{\eta_3} (\tau_3 - \tau_c) = \exp(\alpha t), \quad (24)$$

we obtain the characteristic equation in the form (8) and its roots in the form (9).

Using the solution of (23)

$$\tau = \tau_0 - \vec{\tau}_{1,2} - \frac{\eta_1}{\eta_3} (\tau_3 - \tau_c) + C_1 \exp\left(-\frac{t}{n_1}\right) + C_2 \exp\left(-\frac{t}{n_2}\right) + \eta_1 v \quad (25)$$

and the initial conditions

$$t = 0, \quad \tau(0) = \tau_3 - \vec{\tau}_{1,2}, \quad \dot{\tau}(0) = \mathfrak{G}_\infty v, \quad (26)$$

we find

$$\begin{aligned} \tau = & \tau_0 - \vec{\tau}_{1,2} - \frac{\eta_1}{\eta_3} (\tau_3 - \tau_c) + \left\{ \left( 1 + \frac{\eta_1}{\eta_3} \right) \tau_3 - \tau_0 - \frac{\eta_1}{\eta_3} \tau_c - \eta_1 v \right. \\ & \left. - \frac{n_1 n_2}{n_2 - n_1} \left[ \mathfrak{G}_\infty v + \frac{1}{n_1} \left( \tau_3 + \tau_3 \frac{\eta_1}{\eta_3} - \tau_0 - \frac{\eta_1}{\eta_3} \tau_c - \eta_1 v \right) \right] \right\} \\ & \times \exp\left(-\frac{t}{n_1}\right) + \frac{n_1 n_2}{n_2 - n_1} \left\{ \mathfrak{G}_\infty v + \frac{1}{n_1} \left[ \tau_3 \left( 1 + \frac{\eta_1}{\eta_3} \right) - \tau_0 - \frac{\eta_1}{\eta_3} \tau_c - \eta_1 v \right] \right\} \exp\left(-\frac{t}{n_2}\right) + \eta_1 v. \end{aligned} \quad (27)$$

For the second overloading variant (Fig. 3b) in the section MA ( $\tau_c < \tau < \tau_3$ )

$$\tau - \vec{\tau}_{1,2} - \tau_c + \left( \frac{\eta_3}{\mathfrak{G}_1} + \frac{\eta_2 \eta_3}{\mathfrak{G}_2 \eta_1} + \frac{\eta_3}{\mathfrak{G}_2} + n_2 \right) \dot{\tau} + n_2 \frac{\eta_3}{\mathfrak{G}_1} \ddot{\tau} = \eta_3 v. \quad (28)$$

Taking  $\tau - \vec{\tau}_{1,2} - \tau_c = \exp(\alpha t)$  and proceeding by analogy with the cases presented above for the first initial condition  $\tau(0) = \tau_3 - \vec{\tau}_{1,2}$  [the second one remains the same as in (12), (18), and (26)], we find the solution of (28):

$$\begin{aligned} \tau &= \vec{\tau}_{1,2} + \tau_c + \left\{ \tau_3 - 2\vec{\tau}_{1,2} - \tau_c - \frac{n_1^* n_2^*}{n_2^* - n_1^*} \left[ \mathfrak{G}_\infty v - \frac{1}{n_1^*} \right. \right. \\ &\quad \left. \left. \times (2\vec{\tau}_{1,2} + \tau_c + \eta_3 v - \tau_3) \right] \right\} \exp\left(-\frac{t}{n_1^*}\right) + \left\{ \frac{n_1^* n_2^*}{n_2^* - n_1^*} \right. \\ &\quad \left. \times \left[ \mathfrak{G}_\infty v - \frac{1}{n_1^*} (2\vec{\tau}_{1,2} + \tau_c + \eta_3 v - \tau_3) \right] \right\} \exp\left(-\frac{t}{n_2^*}\right) + \eta_3 v. \end{aligned} \quad (29)$$

In the section AN ( $\tau_0 < \tau < \tau_c$ )

$$\begin{aligned} AP &= \frac{AB}{\eta^*} = \frac{|\vec{\tau}_{1,2}|}{\eta^*}; \\ \Delta\tau &= AC = AP\eta_1 = \frac{|\vec{\tau}_{1,2}| \eta_1}{\eta^*} = |\vec{\tau}_{1,2}| \left(1 + \frac{\eta_1}{\eta_3}\right). \end{aligned}$$

The equation for the unloading along AN is

$$\tau - \tau_0 + \vec{\tau}_{1,2} \left(1 + \frac{\eta_1}{\eta_3}\right) + \left[n_1 + n_2 \left(1 + \frac{\eta_1}{\eta_2}\right)\right] \dot{\tau} + n_1 n_2 \ddot{\tau} = \eta_1 v. \quad (30)$$

Taking  $\tau - \tau_0 + \vec{\tau}_{1,2} [1 + (\eta_1/\eta_3)] = \exp(\alpha t)$  and using  $\tau(0) = \tau_c$  as the first initial condition [the second one remains the same as in (12), (18), and (26)], we obtain the solution of (30) in the form

$$\begin{aligned} \tau &= \tau_0 - \vec{\tau}_{1,2} \left(1 + \frac{\eta_1}{\eta_3}\right) + \left\{ \tau_c - \tau_0 + \vec{\tau}_{1,2} \left(1 + \frac{\eta_1}{\eta_3}\right) - \eta_1 v \right. \\ &\quad \left. - \frac{n_3^* n_4^*}{n_4^* - n_3^*} \left[ \mathfrak{G}_\infty v + \frac{1}{n_3^*} \left( \tau_c - \tau_0 + \vec{\tau}_{1,2} + \vec{\tau}_{1,2} \frac{\eta_1}{\eta_3} - \eta_1 v \right) \right] \right\} \exp\left(-\frac{t}{n_3^*}\right) + \frac{n_3^* n_4^*}{n_4^* - n_3^*} \left[ \mathfrak{G}_\infty v + \frac{1}{n_3^*} \right. \\ &\quad \left. \times \left( \tau_c - \tau_0 + \vec{\tau}_{1,2} + \vec{\tau}_{1,2} \frac{\eta_1}{\eta_3} - \eta_1 v \right) \right] \exp\left(-\frac{t}{n_4^*}\right) + \eta_1 v. \end{aligned} \quad (31)$$

The proposed rheological model (Fig. 1) reflects the "shelf" at the maximum value of  $\dot{\gamma} = \text{const} = v$  obtained in our experiments on a cement test with the repeated application of  $\dot{\gamma}_{\text{max}}$ . Such a "shelf" was also observed in the tests of other authors, such as [7].

The procedure for determining the rheological characteristics entering into Eqs. (27) and (31) does not differ from that described in the preceding section.

### Area of Thixotropy Loop

For the first unloading variant (Fig. 3a)

$$\begin{aligned} S_{DCEN} &= DC \ DN \sin \beta = \frac{(\tau_3 - \vec{\tau}_{1,2} - \tau_0 + \Delta\tau) \Delta\tau}{\eta_1}, \\ S_{APE} &= S_{BPE} - S_{ABP} = \frac{(\tau_3 - \tau_c)^2 (\eta_1 + \eta_3)}{2\eta_3^2}, \\ S_{\text{thixotr.I}} &= S_{DCEN} - S_{APE} = \frac{2\eta_3^2 \left[ \vec{\tau}_{1,2} + \frac{\eta_1}{\eta_3} (\tau_3 - \tau_c) \right] \left[ \tau_3 - \tau_0 + \frac{\eta_1}{\eta_3} (\tau_3 - \tau_c) \right] - \eta_1 (\eta_1 + \eta_3) (\tau_3 - \tau_c)^2}{2\eta_1 \eta_3^2}. \end{aligned} \quad (32)$$

For the second unloading variant (Fig. 3b), using the obvious equality  $S_{\text{thixotr.II}} + S_{\text{NACK}} - S_{\text{BCL}} + S_{\text{AMBD}}$ , we arrive at the expression

$$S_{\text{thixotr.II}} = \frac{2\eta_3^2 \left[ \tau_0 - \vec{\tau}_{1,2} \left(1 + \frac{\eta_1}{\eta_3}\right) \right] \left[ \tau_c - \vec{\tau}_{1,2} \left(1 + \frac{\eta_1}{\eta_3}\right) \right] - \eta_1 \vec{\tau}_{1,2} (\eta_1 + \eta_3)}{2\eta_3^2 \eta_1} + \frac{\vec{\tau}_{1,2} (\tau_3 - \vec{\tau}_{1,2} - \tau_c) (\eta_1 + \eta_3)}{\eta_1 \eta_3}. \quad (33)$$

The area of the figure in the  $\tau - \dot{\gamma}$  axes has the physical meaning of power per unit volume. In [8] it is treated as the power required to accomplish steady flow, and is comprised of the power required to maintain Newtonian flow with  $\dot{\gamma} = \dot{\gamma}_1$  and of the power required to destroy the structure of a consistent medium at the

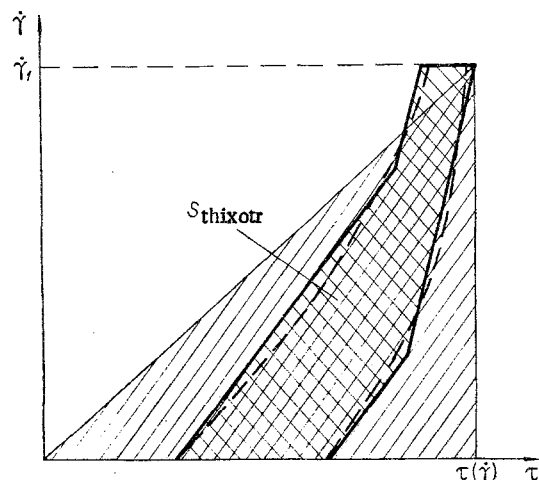


Fig. 4. Diagram of calculation of the coefficient of specific thixotropy area. Dashed line) experimentally determined thixotropy area, replaced by the polygonal area when using the least-squares method, in accordance with Fig. 3a, b.

same value of  $\dot{\gamma} = \dot{\gamma}_1$ . In the present report this specific power characterizes the "memory" of the medium for the previous mechanical action, in the given case, to the stepwise increase in  $\dot{\gamma} = \text{const}$  along the NPA branch of Fig. 3a or the KLD branch of Fig. 3b, while the numerical value of the thixotropy is proportional to the numerical value of this "memory."

In our experiments in determining the thixotropy area of a cement mixture containing crushed sand in a ratio of 1.5:1 by weight and a water content of 0.35 of the weight of dry components ( $\dot{\gamma} = \text{const}$  was varied in the range of 1-530  $\text{sec}^{-1}$  using a Rheotest RV rotary viscosimeter) the specific power (the area of the thixotropy loop) was  $2 \cdot 10^{-4} \text{ J} \cdot \text{sec}^{-1} \cdot \text{m}^{-3}$ .

However, the absolute value of the specific power is insufficiently informative by itself. We therefore introduce the concept of the "coefficient of specific thixotropy area"  $s_{\text{sp}}$ ,

$$s_{\text{sp}} = \frac{S_{\text{thixotr}}(\dot{\gamma}_1)}{0.5\tau\dot{\gamma}_1}, \quad (34)$$

which represents the ratio of the area of the thixotropy loop at the ordinate  $\dot{\gamma}_1$  of the "shelf" to the area characterizing the power required to maintain Newtonian flow (Fig. 4). This coefficient (its value is 0.16 in our experiment) characterizes the contribution of the thixotropic structure destruction to the viscoplastic flow of the medium.

#### NOTATION

$\tau, \gamma$ , shear stress and shear strain;  $\dot{\gamma}_{\text{est II}}$ , established flow velocity in the section  $\tau_c < \tau < \tau_d$ ;  $t$ , time;  $\eta_1, \eta_2, \eta_3, \eta^*$ , greatest plastic viscosity of practically undestroyed structure, viscosity of elastic lag, viscosity of start of structure destruction, and plastic viscosity of structure destruction, respectively;  $n_1 = \eta_1/\mathcal{G}_1$ , stress relaxation time;  $n_2 = \eta_2/\mathcal{G}_2$ , delay (retardation) time of elastic strain;  $\mathcal{G}_1, \mathcal{G}_2, \mathcal{G}_\infty = \mathcal{G}_1\mathcal{G}_2/(\mathcal{G}_1 + \mathcal{G}_2)$ , shear moduli of instantaneous and lag elasticity and long-term elastic shear modulus;  $n_1^*, n_2^*, n_3^*, n_4^*$ , reduced coefficients of relaxation - retardation phenomena;  $\tau_0, \tau_c, \tau_d, \bar{\tau}_1, \bar{\tau}_2$ , plasticity limits of start of flow of practically undestroyed structure, of start of structure destruction, of end of structure destruction (start of emergence onto Newtonian section), and generalized St. Venant elements in Hooke and Kelvin elements of model in Fig. 1;  $\bar{\tau}_{1,2}$ , maximum value of  $\bar{\tau}$  for Hooke and Kelvin elements;  $\tau_3$ , current value of stress in the section  $\tau_c < \tau < \tau_d$  of structure destruction.

#### LITERATURE CITED

1. G. Ya. Kunnos and V. Ē. Mironov, "Method of investigating the rheological properties of foam - concrete mixtures with a nonlinear flow character and influence of swelling temperature on it," in: Technological Mechanics of Concrete. Intercollegiate Scientific - Technical Handbook, Part 3 [in Russian], Rihzskii Politekh. Inst., Riga (1978), p. 40.

2. G. Ya. Kunnos, V. S. Sutkevich, V. G. Khorometskii, A. K. Gailis, and R. A. Kaupas, "Strain and strength properties of foam - concrete adobe, Rheology of concrete mixtures and its technological problems," Summaries of Reports of Second All-Union Symposium [in Russian], Rizhskii Politekh. Inst., Riga (1976), p. 70.
3. G. Ya. Kunnos and U. N. Pall', "Influence of normal stress on creep during simple shear of foam - concrete adobe," Summaries of Reports of Second All-Union Symposium [in Russian], Rizhskii Politekh. Inst., Riga (1976), p. 73.
4. U. N. Pall' and G. Ya. Kunnos, "Strength - strain characteristics of gas - concrete adobe under shear and bending," Tr. Nauchno-Issled. Proektn. Inst. Silikatobetona, No. 12, Tallin, 51 (1978).
5. G. Ya. Kunnos, "Rheological models of bodies with different viscoplastic characteristics in the process of loading and unloading," in: Technological Mechanics of Concrete. Intercollegiate Scientific - Technical Handbook [in Russian], Part 3, Rizhskii Politekh. Inst., Riga (1978), p. 52.
6. I. M. Belkin, G. V. Vinogradov, and A. I. Leonov, Rotary Instruments. Measurement of Viscosity and Physicomechanical Characteristics of Materials [in Russian], Mashinostroenie, Moscow (1968).
7. I. T. Simeonov, Ya. P. Ivanov, and E. D. Stanoeva, "Investigation of the thixotropic properties of cement pastes," in: Reports to Seventh All-Union Conference on Colloid Chemistry and Physicochemical Mechanics [in Russian], Nauka i Tekhnika, Minsk (1977).
8. N. V. Mikhailov and A. M. Likhtgeim, Kolloid. Zh., 17, No. 2, 364 (1955).

#### OPTIMIZED COMPOUND CURRENT LEADS

V. K. Litvinov, V. I. Kurochkin,  
and V. I. Karlashchuk

UDC 536.483

A method is given that provides an acceptable approximation to minimizing the energy consumption on the basis of the finite heat-transfer coefficient and the additional heat sources.

Economy and reliability of the current leads are frequently the decisive factors in the design of a cryogenic magnet system. Here we present some results from theoretical studies on optimized leads that enable one to implement designs providing maximum economy and reliability at the drafting stage.

Detailed studies have been made [1-5] on current leads by means of the recuperation coefficient  $\beta$ , which represents the criterion for nonideal cooling. It is assumed that the recuperation coefficient is known from experiment for leads of constant cross section and that the value is in the range  $0.5 \leq \beta < 1$ ; the heat-transfer coefficient defines the actual cooling process, and this can be used in a method in which  $\beta$  is a specified criterion for minimizing the energy consumption [6]. Then the recuperation coefficient is governed by the specified temperature differences along the normal part of the current lead. The method allows one to use a specified deviation from minimum energy consumption in calculating the geometrical parameters of the lead when this is of variable cross section and the local heat-transfer coefficients are known.

We consider the heat-balance equation for a lead in the stationary one-dimensional approximation [1-5]:

$$\frac{dq}{dT} = c_p m \frac{dT_r}{dT} - \frac{I^2 \rho \lambda}{q}, \quad (1)$$

$$\frac{dx}{dT} = \frac{\lambda S}{q} \quad (2)$$

and the expression for the current dimensions, which is derived by transforming (2) in conjunction with the equation for the heat balance involving the cooling vapor in the steady-state one-dimensional approximation.

We also assume that the thermal conductivity of the cooling vapor is negligible and that the heat-transfer conditions are identical over the entire surface of the lead:

---

Technical Physics Institute, Academy of Sciences of the Ukrainian SSR, Donetsk. Translated from *Inzhenerno-Fizicheskii Zhurnal*, Vol. 37, No. 2, pp. 360-365, August, 1979. Original article submitted June 13, 1978.